Plant Stress 14 (2024) 100618

Contents lists available at ScienceDirect

Plant Stress

journal homepage: www.sciencedirect.com/journal/plant-stress

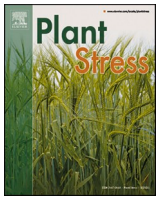

Inositol hexakisphosphate (IP_6) enhances the electrical excitability of Characean *Nitellopsis obtusa*☆

Vilmantas Pupkis *, Judita Janužaitė, Indrė Lapeikaitė, Vilma Kisnierienė

Department of Neurobiology and Biophysics, Institute of Biosciences, Life Sciences Center, Vilnius University, 7 Saulėtekio Ave, Vilnius LT-10257, Lithuania

ARTICLE INFO

Keywords:
Plant action potential
Ca^{2+} channels
Nitellopsis obtusa
Inositol trisphosphate
Inositol hexakisphosphate
Excitation threshold

ABSTRACT

Despite the importance of action potentials (APs) in plant stress physiology, the molecular identity of Ca^{2+} channels that initiate APs by passing Ca^{2+} into the cytoplasm is still unknown in Characean macroalgae. While the Thiel-Beilby mathematical model of AP generation proposes that Ca^{2+} channels are activated by inositol 1,4,5-trisphosphate (IP_3), this hypothesis is controversial because plants do not possess animal IP_3 receptor gene homologues. In the present study, we employed the two-electrode current/voltage clamp technique to determine whether IP_3 and another inositol phosphate IP_6 could modulate the electrogenic parameters of an aquatic macrophyte *Nitellopsis obtusa* internodal cells. IP_3 had no significant effect, whereas IP_6 reversibly hyperpolarised the AP excitation threshold which is consistent with the activation of Ca^{2+} channels. IP_6 also shifted the reversal potentials of the Ca^{2+} and Cl^- currents during excitation to negative membrane potential values, indicating altered calcium dynamics in the cytoplasm. These findings suggest the regulation of Ca^{2+} channels during electrical excitation by IP_6 rather than IP_3. IP_6-induced shift of Ca^{2+} channel voltage dependence allows a lower magnitude external stressor to initiate electrical signalling, thus turning on various downstream physiological responses.

1. Introduction

Inter- and intracellular communication in plants demands faster means than chemical signals; thus, Action Potentials (APs) execute the rapid transmission of information regarding a local stressor to the distal parts of a plant. Propagating APs modulate vital physiological functions such as photosynthetic activity and stress hormone production (Beilby, 2007; Król et al., 2010; Vodeneev et al., 2016).

The underlying principles of the generation of APs are already well-established – after the increase in the cytoplasmic Ca^{2+} concentration, activated Cl^- channels facilitate Cl^- ion efflux. Both these currents, as well as the suppressed activity of H^+-ATPase, rapidly depolarise the membrane potential. Subsequently, activated K^+ channels and restored activity of the proton pump repolarise the membrane to its resting potential value (Lunevsky et al., 1983; Vodeneev et al., 2016).

Although the molecular identity of the above-mentioned membrane transporters has been indicated in *Dionaea muscipula* (Hedrich and Kreuzer, 2023; Scherzer et al., 2022a) it remains the sole plant species with a fully analysed molecular inventory required for electrogenesis. Initial depolarising Ca^{2+} currents are mainly attributed to glutamate receptor-like (GLR) channel activity in higher plants (Mousavi et al., 2013; Scherzer et al., 2022b). In contrast, although Characean macroalgae are able to generate prominent APs and respond electrophysiologically to externally applied amino acids (Lapeikaitė et al., 2020, 2019), their genomes do not possess GLR genes (Nishiyama et al., 2018).

Thus, despite the external similarities of APs in Characean algae and *Dionaea*, their AP generation mechanisms should involve membrane transport systems with low homology, if any.

Decades of functional *in vivo* studies of Characean electrical excitation have allowed the development of the Thiel-Beilby mathematical model of AP generation (Beilby and Al Khazaaly, 2016; Biskup et al., 1999; Kisnieriene et al., 2019; Wacke et al., 2003). The model follows a paradigm valid in animal systems: a cell electrical excitation is initiated due to the activity of 4-state Ca^{2+}-permeable channels located in the endoplasmic reticulum, which are activated by a second messenger and Ca^{2+} and are blocked by additional Ca^{2+}, thus enabling the activation-inactivation dynamics of Ca^{2+} waves. In animal cells, this second messenger is D-*myo*-inositol 1,4,5-trisphosphate (IP_3) which is

☆ This article is part of a special issue entitled: "Ca^{2+} Signaling in Plant Defense: From Cellular to Molecular Level" published at the journal Plant Stress.

* Corresponding author.
E-mail address: vilmantas.pupkis@gmc.vu.lt (V. Pupkis).

https://doi.org/10.1016/j.stress.2024.100618
Received 16 July 2024; Received in revised form 2 September 2024; Accepted 24 September 2024
Available online 28 September 2024

synthesised by a membrane-bound phospholipase C (Othmer, 1997). After adjusting to the plant systems, the predictions of the model were confirmed by experimental results (Wacke et al., 2003).

Despite the success of this model in describing AP alterations under salinity stress in *Chara corallina* (Beilby and Al Khazaaly, 2017, 2016) and *Nitellopsis obtusa* (Kisnieriene et al., 2019), the involvement of IP_3 in the electrogenesis of Characean algae has been questioned (Tazawa and Kikuyama, 2003). Moreover, genes homologous to animal IP_3 receptors have not been identified in Characean algae, or any streptophyte genome (Edel et al., 2017; Krinke et al., 2007).

It has been suggested that while in animals IP_3 acts as a second messenger *per se*, in plants, the reported physiological responses to IP_3 treatment could be caused by its internally phosphorylated product inositol hexakisphosphate (phytic acid, IP_6) (Lemtiri-Chlieh et al., 2003, 2000; Munnik and Testerink, 2009). IP_6 is known to be employed for phosphorus storage in seeds, but it has also been linked to various signalling pathways (Raboy, 2003). For example, IP_6 is a vital precursor of inositol pyrophosphates IP_7 and IP_8, which are involved in the sensing of inorganic phosphate status within plant cells (Freed et al., 2020). IP_6 also binds to the auxin receptor TIR1 (Tan et al., 2007), blocks K_{in} channels, and releases Ca^{2+} from internal stores of *Vicia faba* guard cells (Lemtiri-Chlieh et al., 2003, 2000), but does not affect anion currents (Levchenko et al., 2005).

Due to the unique morphology (Fig. 1), aquatic macrophyte *N. obtusa* together with other Characean algae constitutes a valuable model system in exploring plant physiological functions. Apart from its applicability for photosynthesis research (Navickaite et al., 2024), this alga is of great ecological importance because of its role as an invasive species in the Great Lakes region of the United States (Larkin et al., 2018). This species has also been pivotal in deciphering the functions of various membrane transport systems, their involvement in responses to saline stress, and the role of bioactive compounds in electrical excitation (Kisnieriene et al., 2019).

The involvement of inositol phosphates in plant electrical signalling, especially their effect on Ca^{2+} channels, remains controversial and underexplored. Thus, employing classical electrophysiological techniques, we analysed whether inositol phosphates IP_3 and IP_6 can modulate the electrogenic parameters of the Characean macroalgae *N. obtusa*. We hypothesised that an activator of Ca^{2+} channels would make the cells more excitable, which should be revealed in the alterations of the selected electrogenic parameters.

2. Materials and methods

2.1. Plant material

Intact thalli of the Characean macroalgae *N. obtusa* (N.A. Desvaux) J. Groves were collected from Lithuanian lake Stanka during autumn months and maintained at room temperature (21±1 °C) in glass aquaria under controlled illumination conditions (9.5 ± 0.2 μmol m^{-2} s^{-1}) with a white light/dark photo regime of 12/12 h. Experiments were conducted on internodal cells that were separated from thalli and kept overnight in buffered artificial pond water (APW) under the same illumination conditions (Kisnierienė et al., 2012; Lapeikaitė et al., 2019).

2.2. Solutions

The control solution APW contained 0.1 mM KCl, 1.0 mM NaCl, 0.1 mM $CaCl_2$, 3 mM HEPES, and 1.5 mM Tris (pH 7.2).

The effect of La^{3+} ions was tested employing a solution of 0.5 mM $LaCl_3$ dissolved in APW.

D-myo-inositol 1,4,5-trisphosphate (IP_3) trisodium salt solutions (75 μM and 150 μM) in APW were prepared. To avoid excessive Na^+ concentration, some NaCl was replaced with HCl.

Similarly, a D-myo-inositol hexakisphosphate (IP_6) dodecasodium salt solution (75 μM) in APW was prepared. Since the 150 μM IP_6 solution contains an additional 1,8 mM Na^+ ions, an APW solution supplemented with 1,8 mM Na^+ was used as a control when investigating the effect of this concentration.

The effect of the phospholipase C inhibitor U73122 was investigated employing a 25 μM solution. The substance was first dissolved in DMSO (final concentration 1 %) and then in APW.

All the described solutions were adjusted to pH 7.2. All chemicals were of analytical grade (purchased from Sigma-Aldrich).

2.3. Electrophysiological setup

Electrophysiological experiments using the two-electrode current clamp and voltage clamp techniques were performed as previously described (Fig. 2) (Lapeikaitė et al., 2020, 2019; Pupkis et al., 2022). An internodal cell was placed in a recording chamber filled with the control solution APW (Control-1). A glass microelectrode (1 μm tip) made from borosilicate glass capillaries (Kwik-Fill, World Precision Instruments Inc.) and filled with 3 M KCl solution was inserted using a micromanipulator PatchMan (Eppendorf) into the vacuole of the cell. This 5 mm

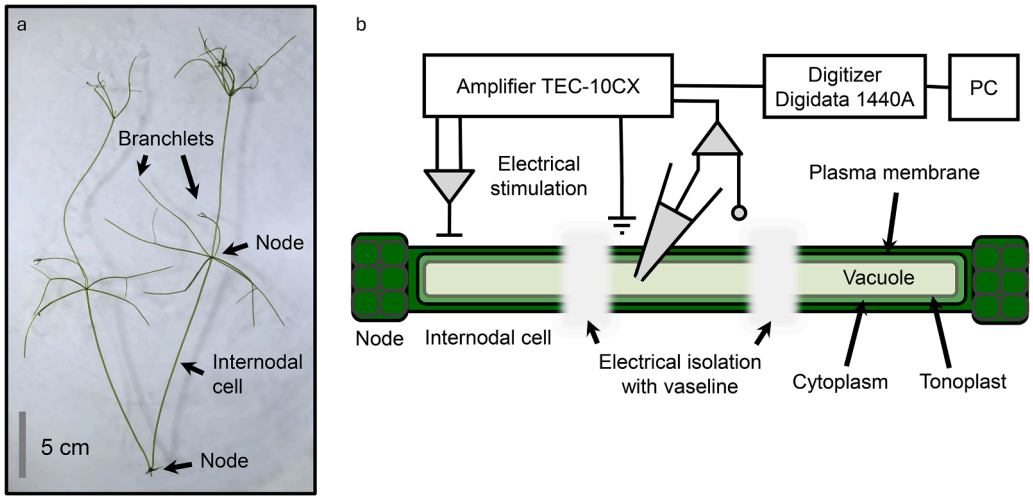

Fig. 1. Apical part of *N. obtusa* thallus with main morphological features highlighted (a); a schematical representation of the electrophysiological setup (b). Intracellular and reference electrodes enable recording of the potential difference across both the plasmalemma and the tonoplast. Separate circuit of extracellular electrodes are used for electrical stimulation.

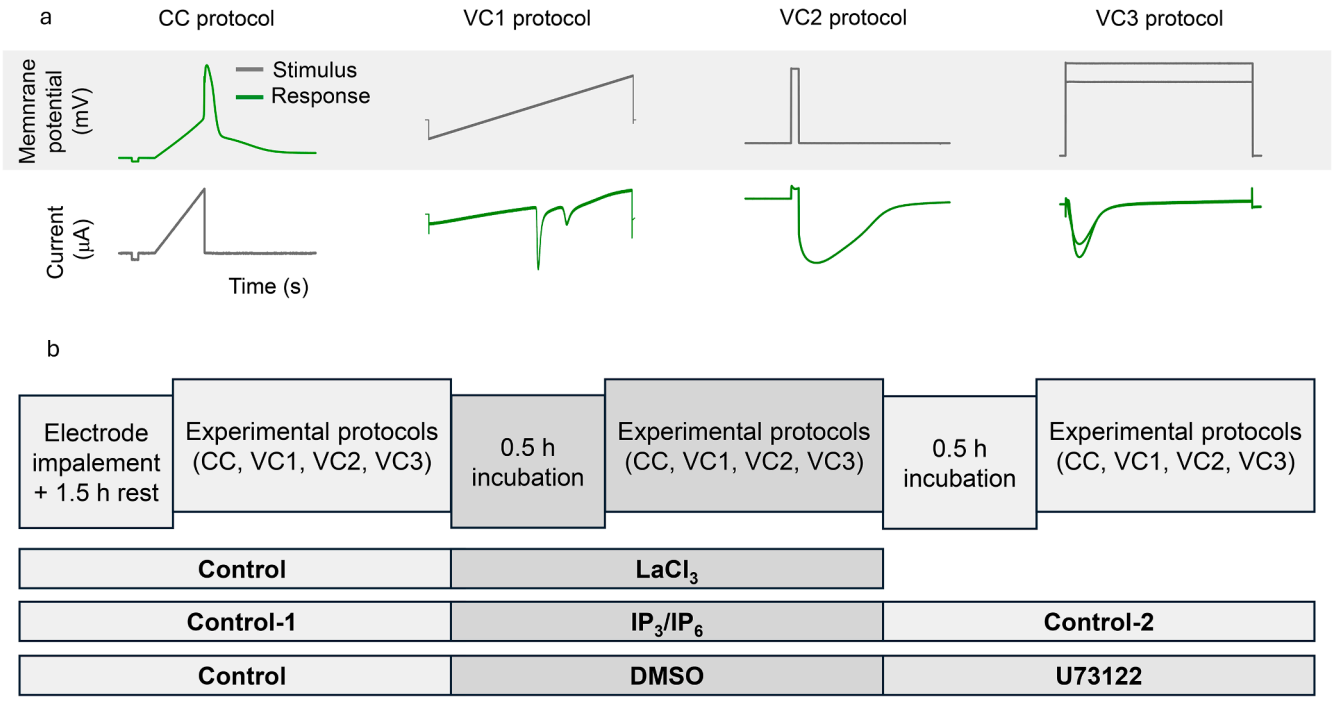

Fig. 2. Applied experimental procedures. Schematic representations of current/voltage protocols (a) employing current/voltage clamp techniques. Stimuli/responses are not to the same scale. Experimental workflow with used substances indicated below (b).

cell region around the intracellular electrode was isolated from the rest of the cell with vaseline and constantly perfused (~1 ml/min; Scientifica PPS system). The reference electrode, filled with a 3 M KCl solution in agar, was placed in the vicinity of the cell near the intracellular microelectrode. The current (DC) was injected using separate extracellular Ag/AgCl electrodes placed near the intracellular electrode and adjacent to the electrically isolated region of the cell. The signal acquisition system consisted of an amplifier TEC-10CX, a digitizer Digidata 1440A, and was controlled using a PC with pCLAMP 10.2 software (Molecular Devices).

2.4. Experimental protocols and evaluated parameters

1.5 h after cell impalement, two APs were stimulated in 5-min intervals (CC protocol). APs were evoked by increasing the direct current at a 0.02 μA/s ramp rate. Once the AP excitation threshold potential (E_{th}) was reached, the stimulation current was terminated.

The membrane resting potential (*RP*) was measured before each AP was evoked. The membrane conductance at rest (G_{RP}) was calculated using Ohm's law when a short rectangular hyperpolarising current pulse (2 s, 50 nA) was applied before each AP was evoked. The E_{th} of an AP was determined as the membrane potential (MP) with a depolarisation rate exceeding 60 mV/s. The AP amplitude was calculated from the E_{th} to the AP peak potential. AP depolarisation duration t_{dep} was evaluated between the E_{th} and the AP peak potential. AP repolarization duration t_{rep} was evaluated between the AP peak potential and the MP repolarized by 90 mV.

After the current clamp protocol, the isolated membrane part of the central cell region was clamped at −180 mV and one or several voltage clamp protocols (depending on the aim) were carried out.

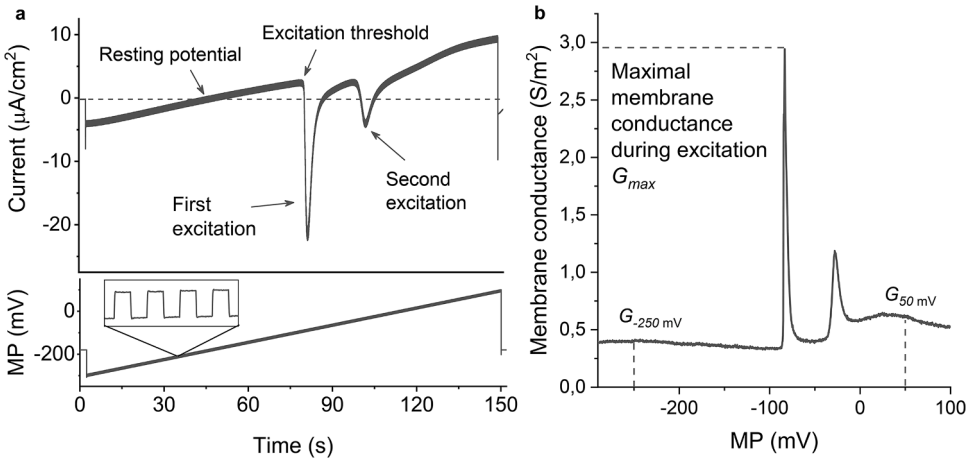

Fig. 3. *N. obtusa* internodal cell electrophysiological parameters registered using the voltage clamp protocol VC1: a) the membrane potential was ramped from −300 mV to 150 mV, this ramp was modulated by rectangular pulses, and the transmembrane currents were recorded; b) according to Ohm's law, the G/V curve was calculated. For statistical analysis, the maximal conductance during excitation G_{max}, as well as membrane conductance at −250 mV ($G_{-250\ mV}$) and at 50 mV were selected ($G_{50\ mV}$).

Three types of voltage clamp protocols were applied. The first, VC1 protocol (Fig. 3), was employed to obtain the membrane conductance values at the selected MP values (G/V curve). For this purpose, the MP was ramped from −300 mV to 150 mV at a velocity of 3 mV/s (Fig. 3a). It has been established that when the ramp velocity is lower than 100 mV/30 s, the I/V curve (except for the excitation transient region) does not differ from the traditional steady-state I/V curves obtained by applying rectangular voltage steps (Tsutsui et al., 1987a). This VC protocol also enables the evaluation of the *RP* value (no current flows through the membrane) and the E_{th} value (MP at which dV/dI becomes negative). The values of these parameters obtained using the VC1 and CC protocols in this study did not differ.

Additionally, this voltage ramp was modulated by rectangular pulses (50 ms, 10 mV), which enabled the calculation of the membrane conductance over the entire voltage range using Ohm's law (Fig. 3b).

For statistical analysis, the maximal membrane conductance during excitation G_{max} was evaluated, as well as the membrane conductance at −250 mV ($G_{-250\ mV}$) and at 50 mV ($G_{50\ mV}$). At approximately −250 mV *N. obtusa* H^+-ATPase is the most conductive (Beilby et al., 1993; Kisnieriene et al., 2019). In addition, with increasing hyperpolarising voltages, inward-rectifying K^+ channels become activated (Blatt, 2024; Kisnieriene et al., 2019; Kisnierienė et al., 2012). At 50 mV, membrane conductance is dominated by the activity of the outward-rectifying K^+ channels (Blatt, 2024; Kisnieriene et al., 2019).

The second voltage clamp protocol (VC2 protocol, Fig. 4) was employed to evaluate the dynamics of the excitation transients, while the membrane potential was clamped at the resting potential. Because the membrane at rest is the most permeable to K^+ ions and protons, the superposition of these currents during excitation was eliminated. A 400 ms rectangular voltage pulse which reached 50 mV was applied to excite the membrane, subsequently, the membrane potential was immediately re-clamped at the resting potential. This allowed registration of the excitation transients at the resting potential (Zherelova et al., 2009). Such a protocol disregards the fact that individual cells exhibit a range of resting potentials; however, the protocol represents ion fluxes in the cell resting state *in vivo*. For statistical analysis, the amplitude of the excitation transient I_{trans} was evaluated as well as its activation and inactivation durations, t_{act_trans} and t_{inact_trans}. t_{act_trans} was calculated between the moment of stimulation and the peak of the excitation transient, whereas t_{inact_trans} was evaluated between the peak of the excitation transient and the moment when its amplitude decreased by 63 %.

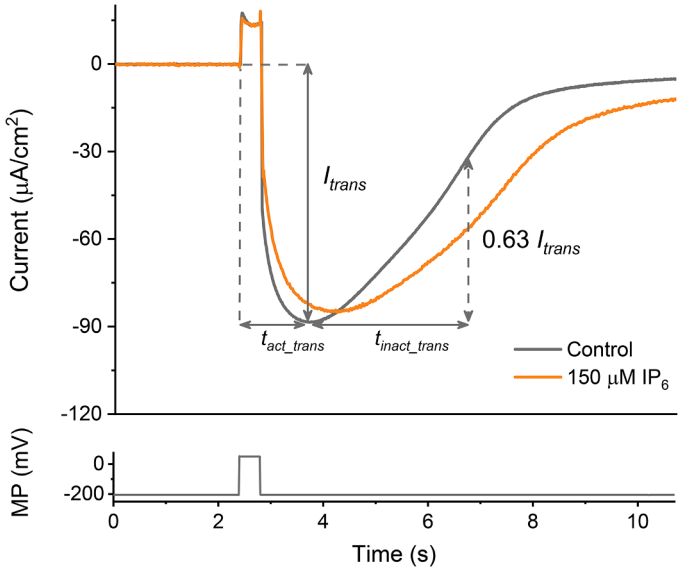

Fig. 4. *N. obtusa* internodal cell electrophysiological parameters registered using voltage clamp protocol VC2. Typical traces of excitation transients of a cell under control conditions and after 30 min exposure to 150 μM IP_6 solution are depicted. The cell membrane potential (MP) was initially clamped at the membrane resting potential; then, for 400 ms, the MP was clamped at 50 mV, and subsequently re-clamped at the resting potential. For statistical analysis, the amplitude of the excitation transient I_{trans} was evaluated as well as its activation and inactivation durations, t_{act_trans} and t_{inact_trans}.

The third voltage clamp protocol (VC3) enabled the evaluation of the amplitudes of the currents constituting the excitation transients and their temporal dynamics at different MP values. A series of rectangular 15 s voltage steps was applied every 3 min. The MP step value was increased by 20 mV for each step, allowing the registration of a series of excitation transients and compilation of the I/V curves (Lapeikaitė et al., 2020, 2019; Pupkis et al., 2022). The evaluated parameters were: the ohmic leakage current I_{leak}, observed after the excitation stimulus for several tens of milliseconds; large inward Ca^{2+} and Cl^- currents I_{Ca} and I_{Cl}, distinguished from current patterns by their temporal characteristics (Ca^{2+} current is initiated first, lasts for several hundred milliseconds, and activates the larger Cl^- current). Subsequently, an outward K^+ current I_K begins to dominate when the excitation transient reaches a steady state. The I_{Cl} activation duration t_{act} (from the initiation of the excitation transient to its peak) and inactivation duration t_{inact} (between the peak of the excitation transient and the moment when its amplitude decreased by 63 %) were also evaluated.

After the voltage clamp protocols were carried out under control conditions (Control-1), the above-mentioned constantly perfused 5 mm region of the cell surface was exposed to the desired experimental solution and incubated for 30 min. The entire procedure consisting of the current clamp and voltage clamp protocols was then repeated. When investigating the effect of IP_3 and IP_6, the cell was re-exposed to the control conditions (Control-2), and the same protocols were carried out. To evaluate the effect of the phospholipase C blocker U73122, a cell was first exposed to the control conditions, then to 1 % DMSO dissolved in the control solution, and finally to U73122 dissolved in DMSO in the control solution.

2.5. Investigation of cyclosis

In Characean cells, the velocity of vigorous cytoplasmic streaming (cyclosis) depends on the cytoplasmic Ca^{2+} concentration: electrical stimulation of a cell releases Ca^{2+} into the cytoplasm, which reversibly locks the actomyosin complex and stops cyclosis (Shimmen, 2007).

In this study, the velocity of cyclosis was examined at rest and after electrical excitation, allowing the observation of its restoration dynamics (Pupkis et al., 2021). The cells were observed employing a microscope Eclipse FN1 with a camera DS-Fi1c (Nikon) at 200× magnification. Visual data were recorded using the OBS Studio program and analysed later. The velocity of cyclosis was calculated every 1 min by recording the time required for a visible cytoplasmic particle to move a certain distance.

During the experiment, an internodal cell was immersed in the control solution (Control-1) for 10 min and then electrically excited using a 1.5 V battery. Cyclosis recovery was observed for 20 min. The cell was then immersed in a 150 μM IP_6 solution and incubated for 30 min. After electrical excitation, cyclosis was observed for 20 min. Finally, the cell was re-immersed in the control solution (Control-2) for 30 min and electrically excited. Cyclosis recovery was observed for 20 min.

The restoration of cyclosis after electrical excitation was approximated using an exponential function (Pupkis et al., 2021), whose parameters v_{max} – maximal velocity of cyclosis and τ – time constant of the restoration, as well as the velocity of cyclosis during rest v_r were chosen for statistical analysis.

2.6. Data analysis

Data were analysed using software pClamp 10.2 (Molecular Devices), MicroCal OriginPro 2018 (OriginLab), and the programming

language R (package *rstatix* 0.7.2 for statistical analysis).

The sample size, n, denotes the number of cells. They were as follows: 0,5 mM $LaCl_3$ – $n = 5$ (CC protocol), $n = 6$ (VC1 and VC2 protocols); 75 μM IP_3 – $n = 6$ (CC protocol), $n = 8$ (VC1 and VC2 protocols); 150 μM IP_3 – $n = 4$ (CC, VC1, and VC2 protocols); 75 μM IP_6 – $n = 9$ (CC protocol), $n = 8$ (VC3 protocol); 150 μM IP_6 – $n = 8$ (CC and VC3 protocols), $n = 4$ (VC1 protocol, investigation of cyclosis), $n = 3$ (VC2 protocol); 25 μM U73122 – $n = 4$ (CC, VC1, and VC2 protocols).

To calculate the reversal potentials of the I_{Ca} and I_{Cl} currents, the I/V of a particular current in a single cell was approximated with a 3rd polynomial whose mathematical solution provided the reversal potential value.

To evaluate whether observed differences between selected parameters were significant, statistical tests were employed. Because the selected parameters were registered on the same cell under different conditions, paired statistical tests were employed. For IP_3, IP_6 and U73122 exposure experiments, repeated measures ANOVA with pairwise paired *t*-tests post-hoc analysis employing Bonferroni multiple testing correction method, or Friedman rank sum test with Wilcoxon signed-rank test post-hoc analysis employing Bonferroni multiple testing correction method, depending on the parameter value distribution (Shapiro-Wilk test). For $LaCl_3$ exposure experiments, paired *t*-test or Wilcoxon signed-rank test was applied depending on the parameter value distribution (Shapiro-Wilk test). To compare the effect of different concentrations of inositol phosphates on the AP excitation threshold, the difference between the E_{th} value in the control conditions and after exposure was calculated (ΔE_{th}). These differences were compared using independent measures ANOVA with Tukey HSD post-hoc analysis employing Tukey multiple testing correction method, as the data were normally distributed (Shapiro-Wilk test).

In all cases, a difference was considered significant at $p < 0.05$. The results are expressed as mean values ± SD.

3. Results

3.1. Ca^{2+} channel blocker La^{3+} depolarizes AP excitation threshol

The inhibitory effects of La^{3+} on plant electrogenesis via action on Ca^{2+} channels have been well documented, with lower concentrations reducing AP amplitude and increasing AP duration (Krol et al., 2006; Shiina and Tazawa, 1987; Tsutsui et al., 1987b), whereas higher concentrations and longer exposure abolish electrical excitation altogether (Scherzer et al., 2022a; Tsutsui et al., 1987a).

As expected, in the present research 30 min exposure of *N. obtusa* internodal cells to 0.5 mM $LaCl_3$ decreased the maximal membrane conductance during excitation G_{max} and the AP amplitude ($p = 0.019$; Table S1). Although the AP peak value was not significantly diminished, the AP excitation threshold E_{th} value was depolarised by approximately 20 mV ($p = 0.047$; Fig. 5, Table S1). Thus, alterations in the AP threshold E_{th} value suggest modulation of Ca^{2+} channel activity.

In several experiments, the cells affected by La^{3+} were re-exposed to the control solution for 30 min. The inhibitory action of La^{3+} was not reversible and often intensified, sometimes leading to a complete loss of cell electrical excitability.

3.2. IP_3 does not significantly affect the electrogenesis of N. obtusa

External exposure of *N. obtusa* cells to 75 μM or 150 μM of IP_3 did not lead to any consistent changes in the selected electrogenic parameter values (Tables S1, S2). The phospholipase C blocker U73122 also did not exert any significant effect (Tables S1, S2). However, it should be noted that after exposure to IP_3, a trend of AP excitation threshold hyperpolarisation was observed in some cells. Under stable control conditions, *N. obtusa* cells virtually never generate spontaneous APs. After exposure to 75 μM IP_3 solution, one cell out of nine, and after exposure to 150 μM IP_3 solution, one out of four generated trains of spontaneous action potentials.

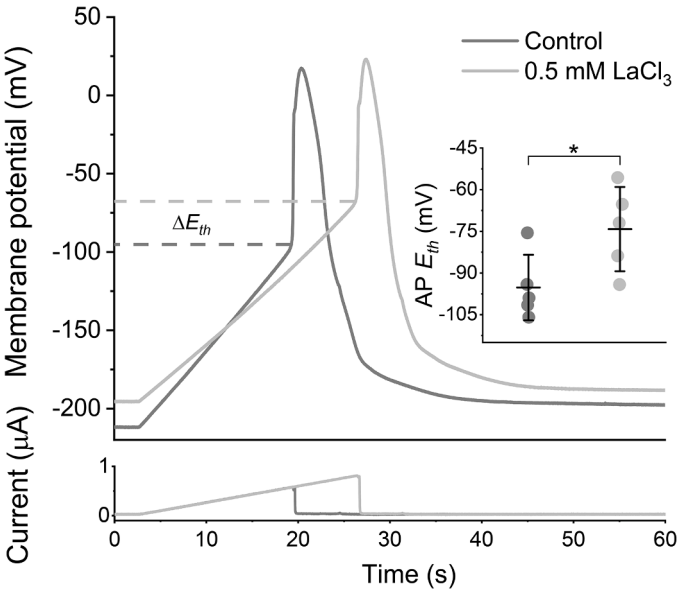

Fig. 5. Representative example of the effect of 30 min exposure to 0,5 mM $LaCl_3$ solution on the electrically-elicited APs of *N. obtusa* internodal cell. The insert represents the AP excitation threshold E_{th} values (mean ± SD) under different conditions. The asterisk indicates a statistically significant difference ($p < 0,05$). $n = 5$.

3.3. IP_6 hyperpolarises AP excitation threshold but does not affect AP amplitude

In contrast to IP_3, the same concentrations (75 μM and 150 μM) of IP_6 significantly affected the electrogenic parameters of *N. obtusa* internodal cells (Fig. 6, Tables 1, 2, S2). External exposure of the cells to 75 μM of IP_6 hyperpolarised the AP excitation threshold by approximately 15 mV ($p = 0.046$). Hyperpolarisation induced by 150 μM of IP_6 was even larger

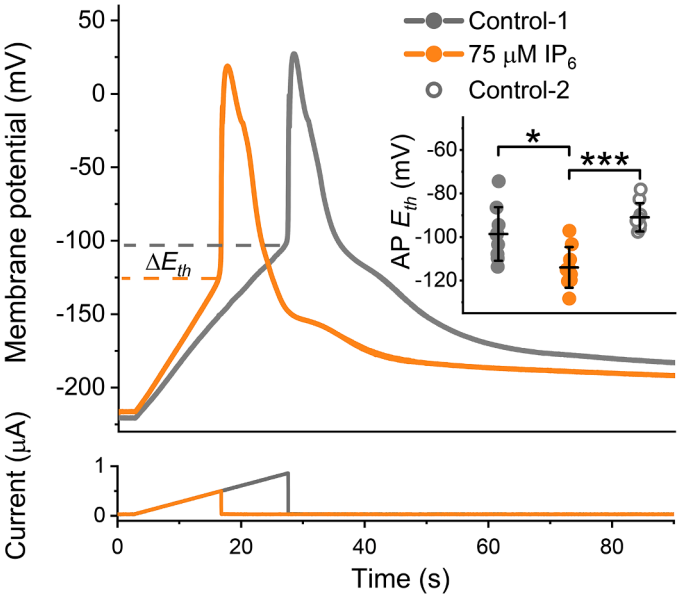

Fig. 6. A representative example of the effect of 30 min exposure to 75 μM inositol hexakisphosphate (IP_6) solution on the electrically-elicited APs of *N. obtusa*. The insert shows the AP excitation threshold E_{th} values (mean ± SD) under different conditions. Control-2 represents re-exposure to the control solution. Asterisks indicate statistically significant differences ($p < 0.05$). $n = 9$.

Table 1
The effect of 75 μM inositol hexakisphosphate (IP_6) on the parameters of electrogenesis of *N. obtusa*, determined using the CC protocol. $n = 9$. Values (means ± SD) presented with asterisks represent significant differences ($p < 0.05$) when compared with Control-1. The underlined values represent significant differences ($p < 0.05$) compared with Control-2 (re-exposure to the control solution).

	Control-1	IP_6 75 μM	Control-2
Resting potential *RP* (mV)	−222±17	−215±17	−216±18
Membrane conductance at rest G_{RP} ($S{\cdot}m^{-2}$)	0.57 ±0.34	0.6 ± 0.44	0.48 ±0.25
AP excitation threshold E_{th} (mV)	−99±12	−114±9*	−91±7
AP peak (mV)	29±7	20±13	31±16
AP amplitude (mV)	128±17	135±14	122±15
AP depolarization duration t_{dep}(s)	1.3 ± 0.3	1.3 ± 0.3	1.2 ± 0.2
AP repolarization duration t_{rep} (s)	3.6 ± 1.3	4.2 ± 1.2	3.3 ± 0.9

Table 2
The effect of 150 μM inositol hexakisphosphate (IP_6) on the parameters of electrogenesis of *N. obtusa*, acquired using the CC, VC1, and VC2 protocols. n = 4–8. Values (means ± SD) presented with asterisks represent significant differences ($p < 0.05$) when compared with Control-1. The underlined values represent significant differences ($p < 0.05$) compared with Control-2 (re-exposure to the control solution).

	Control-1	IP_6 150 μM	Control-2
Resting potential *RP* (mV)	−206 ±19	−195 ±31	−180 ±35
Membrane conductance at rest G_{RP} ($S{\cdot}m^{-2}$)	0.33±0.1	0.34 ±0.11	0.37±0.1
AP excitation threshold E_{th} (mV)	−96±5	−133 ±15*	−89±9
AP peak (mV)	35±9	13±10*	37±11
AP amplitude (mV)	130±10	146±18	125±12
AP depolarization duration t_{dep}(s)	1.2 ± 0.2	1.5 ± 0.4*	1.3 ± 0.2
AP repolarization duration t_{rep} (s)	3.6 ± 1.2	7.2 ± 5.1*	4.1 ± 2
Maximal membrane conductance during excitation G_{max} ($S{\cdot}m^{-2}$)	5.5 ± 1.2	6.8 ± 2.4	4.6 ± 2.3
Membrane conductance at −250 mV $G_{-250\ mV}$ ($S{\cdot}m^{-2}$)	0.41 ±0.05	0.42 ±0.05	0.42 ±0.06
Membrane conductance at 50 mV $G_{50\ mV}$ ($S{\cdot}m^{-2}$)	1.03 ±0.16	1.25 ±0.37	0.99 ±0.27
Excitation transient amplitude I_{trans} ($\mu A{\cdot}cm^{-2}$)	−89±23	−102 ±36	−65±34
Excitation transient activation duration t_{act_trans} (s)	1.2 ± 0.3	1.5 ± 0.3	1.2 ± 0.4
Excitation transient inactivation duration t_{inact_trans} (s)	1.9 ± 0.8	2.8 ± 1	2.2 ± 1

and amounted to approximately 40 mV ($p < 0.001$). The higher concentration of IP_6 hyperpolarised the AP excitation threshold more than the lower concentration, as well as more than either of the IP_3 concentrations (Tables S1, S2).

While the cell exposure to the lower concentration of IP_6 showed only a trend of AP peak value reduction, the exposure to the higher concentration diminished the AP overshoot by approximately 20 mV ($p = 0.001$). Consistent with these results, the AP amplitudes were not affected by either concentration. Cell exposure to 150 μM of IP_6 did not affect the maximal membrane conductance during excitation G_{max} or the excitation transient amplitude I_{trans}, which corresponds to the unchanged AP amplitude values (Tables 2, S2). All these effects were reversible, as the alterations in the parameter values were abolished by re-exposing the cells to the control solution for 30 min (Tables 1, 2, S2).

150 μM of IP_6 also increased both AP depolarisation duration t_{dep} and its repolarization duration t_{rep} (Tables 2, S2).

3.4. IP_6 shifts reversal potentials of the Ca^{2+} and Cl^- currents during excitation

Because IP_6 affected the AP parameter values, a more detailed investigation was carried out using the VC3 protocol.

No effect on the Ca^{2+} current I_{Ca} was observed when the cells were exposed to the lower solution of IP_6. However, cell exposure to 150 μM of IP_6 reversibly shifted the reversal potential of this current by approximately 30 mV to more negative membrane potentials ($p < 0.001$). Thus, at almost all voltages in the interval between −100 mV and 60 mV, the Ca^{2+} current amplitudes were significantly affected. The I/V curve also confirmed that IP_6 hyperpolarizes the excitation threshold (Fig. 6). It should be noted that despite the shift of the I/V curve, the maximal I_{Ca} amplitude (at the excitation threshold) was similar before and after cell exposure to IP_6 (Fig. 7(a), Tables S2, S3).

The effect of IP_6 on the Cl^- current I_{Cl} during excitation was not as pronounced. 75 μM of IP_6 reduced the I_{Cl} amplitude at −40 mV, at −20 mV, and at 40 mV, whereas exposure to 150 μM of IP_6 significantly affected current amplitudes only at 60 mV, indicating a shifted reversal potential in the negative direction ($p = 0.002$; Fig. 7 (b), Tables S2, S3).

While the Cl^- current activation times t_{act} were affected by exposure to 75 μM of IP_6 only at certain voltages, cell exposure to the higher concentration of IP_6 led to reversibly prolonged activation times t_{act} in a voltage range between −80 and 0 mV (Fig. 8(a), Tables S2, S3). Similarly, cell exposure to IP_6 prolonged Cl^- current inactivation times t_{inact}. The lower concentration of IP_6 was significantly effective in the voltage range from −80 mV to −40 mV, while the higher concentration induced a more potent prolongation of t_{inact} in the voltage range from −60 mV to 40 mV (Fig. 8 (b), Tables S2, S3).

The cyclosis assay of *N. obtusa* internodal cell under exposure to 150 μM IP_6 solution did not reveal any significant effect on the analysed cyclosis parameters in either the resting state or after cell electrical excitation (Fig. 9).

4. Discussion

In plants, IP_3 has been linked to the regulation of a number of physiological processes (Krinke et al., 2007), including gravisensing and auxin transport (Perera et al., 2006; Zhang et al., 2011), blue light-induced morphogenesis (Chen et al., 2008), abscisic acid-mediated stomatal closure (Meimoun et al., 2009), and responses to various stressors (Xiong et al., 2001) and stomatal closure (Gilroy et al., 1990). Usually, the implied IP_3 signal transduction pathway includes the elevation of the cytoplasmic Ca^{2+} concentration which links the intracellular IP_3 concentration increase to the tangible physiological outcomes, supposedly via activation of kinases and/or phosphatases (Chen et al., 2008; Gilroy et al., 1990; Zhang et al., 2011). Several reports from the 1990s claimed that IP_3-activated Ca^{2+} channels exist in the vacuolar membrane of *Beta vulgaris* (Alexandre et al., 1990; Allen and Sanders, 1994), however, these results have not been reproduced (Pottosin et al., 2009). Thus, as no animal IP_3 receptor homologues have been reported in plant genomes (Edel et al., 2017; Krinke et al., 2007), the molecular mechanism of IP_3 action remains elusive.

In Characean algae, Ca^{2+} channel activation is linked with the depolarisation phase of APs (Lunevsky et al., 1983; Williamson and Ashley, 1982). IP_3 has been strongly implicated in activating these channels and thus initiating the AP generation (Beilby and Al Khazaaly, 2016; Biskup et al., 1999; Wacke et al., 2003; Zherelova, 1989); however, some of the key experimental results have not been replicated (Tazawa and Kikuyama, 2003). Generally, putative IP_3 receptors are not considered when modelling plant electrical activity, and their theoretical role is reported to be insignificant (Novikova et al., 2017).

In plants, the initial increase in the cytoplasmic Ca^{2+} concentration during the electrogenesis is followed by the larger Ca^{2+}-activated Cl^- efflux (Lunevsky et al., 1983; Williamson and Ashley, 1982). Thus, the AP excitation threshold value could be considered a biomarker

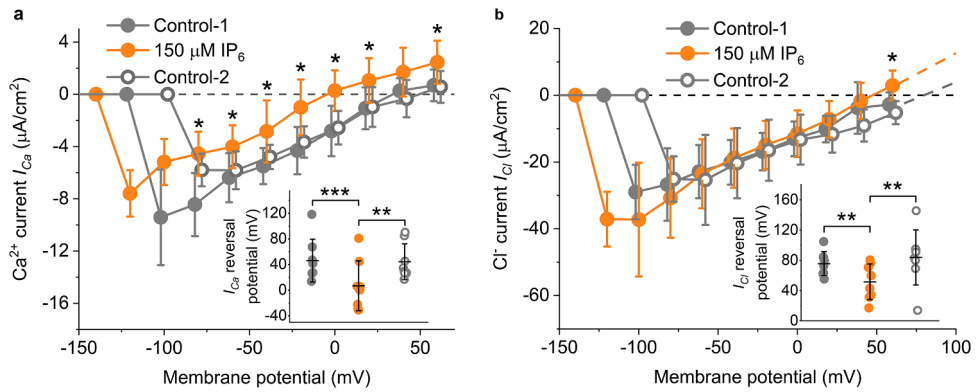

Fig. 7. I/V curves of the Ca^{2+} currents I_{Ca} (a) and Cl^- currents I_{Cl} (b) during the electrical excitation of *N. obtusa* internodal cells under control conditions and after 30 min exposure to 150 μM inositol hexakisphosphate (IP_6) solution. Values are presented as the mean ± SD. Asterisks indicate statistically significant differences ($p <$ 0,05) (in the main graph – between Control-1 and IP_6 groups). $n = 8$. Control-2 represents re-exposure to the control solution. Inserts depict the IP_6-induced shift in the I_{Ca} current (a) and I_{Cl} current (b) reversal potentials.

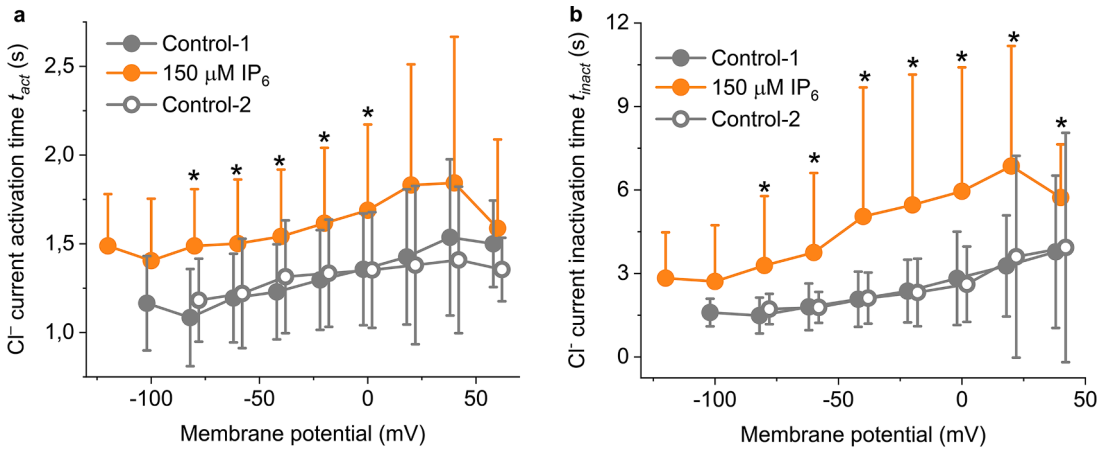

Fig. 8. Activation times t_{act} (a) and inactivation times t_{inact} (b) of the Cl^- current I_{Cl} during the electrical excitation of *N. obtusa* internodal cells under control conditions and after 30 min exposure to 150 μM inositol hexakisphosphate (IP_6) solution. Values are presented as the mean ± SD. Asterisks indicate statistically significant differences ($p <$ 0,05) between Control-1 and IP_6 groups. Control-2 represents re-exposure to the control solution. $n = 8$.

characterising the activity of the Ca^{2+} channels. In liverworts, amino acids activate Ca^{2+} influx (Koselski et al., 2020; Krol et al., 2007) but it is methodically problematic to determine the AP E_{th} value in this model system as well as in other land plants. In contrast, *N. obtusa* cells exhibit a significant hyperpolarisation of the AP E_{th} after exposure to amino acids. (Lapeikaitė et al., 2020, 2019). Conversely, organic Ca^{2+} channel blockers depolarise the Characean AP E_{th}; however, they also induce non-specific effects (Koselski et al., 2021; Pupkis et al., 2022). La^{3+} has been widely employed as a Ca^{2+} channel blocker in electrophysiological research on plants in many taxa (Koselski et al., 2023; Scherzer et al., 2022a). In the present study, we report that 0.5 mM La^{3+} depolarised the AP E_{th}, further confirming the link between Ca^{2+} channel activity and the AP E_{th}. During the 30 min exposure, we did not observe La^{3+} effect on parameters linked with other ion transport systems (for example H^+-ATPase, K^+ channels) which would have been reflected in parameters such as *RP*, $G_{-250\ mV}$, or $G_{50\ mV}$ (Fig. 5, Table S1). Thus, we interpret the alterations in the AP E_{th} as an indication of modulated Ca^{2+} channel activity, which can be employed to test the effect of inositol phosphates on the electrogenesis of Characean macroalgae.

In this study, *N. obtusa* cells were externally exposed to 75 μM and 150 μM IP_3 solutions. While IP_3 showed some potential in enhancing the cell electrical excitability, no significant alterations in the electrogenic parameters were observed. Intracellular IP_3 is generated by a phospholipase C (PLC) which hydrolyses phosphatidylinositol bisphosphate (PIP_2) to diacylglycerol (DAG) and IP_3. A common approach to lowering the intracellular IP_3 concentration is the application of PLC inhibitors (Biskup et al., 1999; Meimoun et al., 2009). In this study, exposing *N. obtusa* cells to the PLC inhibitor U73122 had no effect on the electrogenic parameters (Tables S2, S3). Thus, we cannot confirm IP_3 as an unequivocal modulator of Characean electrical signalling.

It has been suggested that in plants, the role of IP_3 as a second messenger may be fulfilled instead by another inositol phosphate – IP_6 (Lemtiri-Chlieh et al., 2003, 2000; Munnik and Testerink, 2009). In *Vicia faba* and *Solanum tuberosum*, plasma membrane K^+_{in} channels are blocked by increased intracellular Ca^{2+} concentration. Both IP_3 and IP_6 have been shown to reduce K^+_{in} currents by mobilising Ca^{2+} from internal stores, but the effect of IP_6 is more potent (Lemtiri-Chlieh et al., 2003, 2000). IP_6 also activates slow vacuolar (SV) and fast vacuolar (FV) channels which are Ca^{2+}-permeable (Lemtiri-Chlieh et al., 2003). Based on these results, it has been speculated that cytoplasmic IP_3 might be converted to IP_6 which is the actual second messenger in plants. Consequently, the search for IP_3 receptors should be futile, and rather targets of IP_6 should be sought (Lemtiri-Chlieh et al., 2003, 2000; Munnik and Vermeer, 2010). Alternatively, two separate signalling systems may be employed for the mobilisation of Ca^{2+} to the cytoplasm, one involving IP_3 and the other involving IP_6 (Krinke et al., 2007).

In the present study, in contrast to IP_3, the external application of IP_6 was effective in modulating the electrogenesis of *N. obtusa* internodal cells. The most prominent observation was that IP_6 hyperpolarised the AP excitation threshold E_{th} (Fig. 6, Tables 1, 2, S2) which indicates its

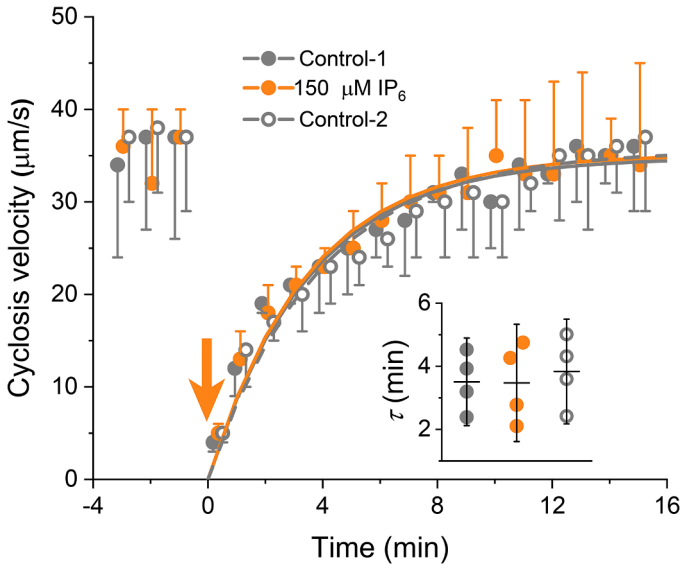

Fig. 9. Velocity of cyclosis in *N. obtusa* internodal cells under control conditions and after 30 min exposure to 150 μM inositol hexakisphosphate (IP_6) solution. The orange arrow indicates the moment of electrical excitation of the cell ($t = 0$). The insert depicts the time constant τ of cyclosis restoration after electrical stimulation. Values are presented as means ± SD. Control-2 represents re-exposure to the control solution. $n = 4$.

action on Ca^{2+} channels responsible for excitation. The Thiel-Beilby model of the Characean AP generation was constructed considering the possibility that not necessarily IP_3, but any molecule, whose kinetics of metabolism are similar to IP_3 may fulfil the function of the Ca^{2+} channel activator (Beilby, 2019; Wacke and Thiel, 2001). Based on our results, this signalling molecule is suggested to be IP_6. To date, there have been no reports of IP_6 receptor genes capable of Ca^{2+} release in either animal or plant model systems (Krinke et al., 2007). Thus, research on *N. obtusa* might reveal a novel inositol phosphate interaction site on Ca^{2+} channels whose molecular properties remain elusive.

Cell exposure to IP_6 also affected other electrophysiological parameters. While the shifted reversal potential of the Ca^{2+} current I_{Ca} indicates an increased cytoplasmic Ca^{2+} concentration (Fig. 7(a), Tables S2, S3), other evidence does not provide a conclusive answer. The velocity of cyclosis at rest was not altered by IP_6 (Fig. 9, Tables S2, S3), in addition, the maximal membrane conductance during excitation G_{max} was not affected by IP_6. IP_6 also had no significant effect on the AP amplitude. The Cl^- current I_{Cl} amplitudes near the excitation threshold and the amplitudes of the excitation transient at rest I_{trans} were also unaffected (Fig. 7 (b), Tables 1, 2, S2, S3). These results indicate that IP_6 does not act on Ca^{2+} channels by increasing their open probability but by shifting their voltage dependence to more hyperpolarised voltages.

IP_6 also prolonged the temporal dynamics of both the APs and excitation transients (Figs. 4, 6, Tables S2, S3). The effect on the AP depolarisation duration t_{dep} and Cl^- current I_{Ca} activation time t_{act} may be linked with altered intracellular Ca^{2+} dynamics and its influence on the Cl^- current. Prolongation of the AP repolarization duration t_{rep} and Cl^- current I_{Ca} inactivation time t_{inact} can also be linked to IP_6 effect on Ca^{2+} transport systems, such as the alteration of Ca^{2+}-ATPase activity, which removes Ca^{2+} from the cytoplasm after excitation. Under the influence of IP_6, or by activation at more negative MP values, the pump might not operate as effectively, which is supported by the shifted I_{Ca} current reversal potential (Fig. 7(a)). The influence of the modulated activity of the H^+ and K^+ transport systems on the above-mentioned parameters should be dismissed, since IP_6 did not affect the membrane resting potential *RP*, membrane conductance at −250 mV $G_{-250\ mV}$, and at 50 mV $G_{50\ mV}$. The K^+ current I_K extracted from the excitation transients was also unaffected. Thus, it can be concluded that IP_6 does not exert an effect on the H^+-ATPase, K^+_{in}, and K^+_{out} channels (Tables 1, 2, S2, S3). The leakage (background) current I_{leak} was also unaffected by IP_6 (Tables S2, S3).

The molecular identity of the Ca^{2+}-permeable channels in *N. obtusa*, specifically those activated by IP_6 in this study, is not clear. While it has been reported that IP_6 activates slow vacuolar (SV) channels (Lemtiri-Chlieh et al., 2003) which are encoded by the two-pore channel (TPC) gene, and Characean algae possess one TPC gene homologue (Nishiyama et al., 2018), SV channel activity has not been recorded in the *N. obtusa* vacuolar membrane (Koselski et al., 2021). The genes encoding the fast vacuolar (FV) channels, which are also reportedly activated by IP_6 (Lemtiri-Chlieh et al., 2003), have not been identified yet (Pottosin and Dobrovinskaya, 2014).

A similar but not identical IP_6 effect pattern on the electrical excitability is exerted by amino acids Asn and Glu as well as the synthetic animal ionotropic glutamate receptor (iGluR) agonist NMDA, which also hyperpolarise the AP E_{th} of *N. obtusa*. (Lapeikaitė et al., 2020, 2019) It is unclear whether these amino acids and IP_6 act on the same target or if there are distinct Ca^{2+} channels modulated by different signalling molecules. This possibility is supported by research in *Phiscomitrium patens*, where GLR knock-out mutants were still able to generate electrical signals, although their amplitude was diminished, indicating the activity of other, non-GLR Ca^{2+}-permeable channels (Koselski et al., 2023).

We tested only two possible Ca^{2+} channel agonists, IP_3 and IP_6, but other inositol phosphates also may have a role in plant electrical signalling. Without the structural data of the Ca^{2+} channels, it is nearly impossible to reliably decipher the regulatory network of inositol phosphates because of their unknown internal turnover kinetics. While the present study does not account for the possible seasonal or individual variations and bases the conclusions on small data samples, the underlying trends robustly support inositol phosphates as possible novel regulators of Ca^{2+} channels.

Hyperpolarisation of the AP excitation threshold indicates that a lower magnitude external stressor is sufficient to initiate electrical signalling, which has profound physiological consequences, such as an earlier production of stress hormones or inhibition of photosynthetic processes (Sukhov et al., 2019). Future work should focus on a more precise observation of calcium waves employing fluorescent indicators, which should be paired with molecular data to pinpoint the exact molecular identity and intracellular localisation of the IP_6-regulated Ca^{2+} channels to gain more mechanistic insights into plant stress signalling.

5. Conclusions

The role of inositol phosphates in altering plant electrical activity has been controversial because of the absence of animal IP_3 receptor gene homologues in plants. The present study could not confirm IP_3 as a second messenger in Characean algae that activates Ca^{2+} channels and initiates the generation of APs. However, another inositol phosphate, IP_6, reversibly hyperpolarised the AP excitation threshold, shifting the voltage dependence of the Ca^{2+} channels and thus increasing the cell excitability. Therefore, IP_6 is a more probable putative second messenger theorised by the Thiel-Beilby mathematical model of the Characean AP generation.

CRediT authorship contribution statement

Vilmantas Pupkis: Writing – review & editing, Writing – original draft, Visualization, Software, Methodology, Investigation, Formal analysis, Conceptualization. **Judita Janužaitė:** Investigation, Formal analysis. **Indrė Lapeikaitė:** Writing – review & editing. **Vilma Kisnierienė:** Writing – review & editing, Supervision, Resources, Conceptualization.

Declaration of competing interest

The authors declare that they have no known competing financial interests or personal relationships that could have appeared to influence the work reported in this paper.

Data availability

Data will be made available on request.

Supplementary materials

Supplementary material associated with this article can be found, in the online version, at doi:10.1016/j.stress.2024.100618.

References

Alexandre, J., Lassalles, J.P., Kado, R.T., 1990. Opening of Ca^{2+} channels in isolated red beet root vacuole membrane by inositol 1,4,5-trisphosphate. Nature 343, 567–570.

Allen, G.J., Sanders, D., 1994. Osmotic stress enhances the competence of *Beta vulgaris* vacuoles to respond to inositol 1,4,5-trisphosphate. Plant J.

Beilby, M.J., 2007. Action potential in charophytes. Int. Rev. Cytol. 257, 43–82.

Beilby, M.J., 2019. *Chara braunii* genome: a new resource for plant electrophysiology. Biophys. Rev. Lett. 11, 235–239.

Beilby, M.J., Al Khazaaly, S., 2016. Re-modeling Chara action potential: I. from Thiel model of Ca^{2+} transient to action potential form. AIMS Biophys. 3, 431–449.

Beilby, M.J., Al Khazaaly, S., 2017. Re-modeling Chara action potential: II. The action potential form under salinity stress. AIMS Biophys. 4, 298–315.

Beilby, M.J., Mimura, T., Shimmen, T., 1993. The proton pump, high pH channels, and excitation: voltage clamp studies of intact and perfused cells of *Nitellopsis obtusa*. Protoplasma 175, 144–152.

Biskup, B., Gradmann, D., Thiel, G., 1999. Calcium release from InsP3-sensitive internal stores initiates action potential in *Chara*. FEBS Lett. 453, 72–76.

Blatt, M.R., 2024. A charged existence: a century of transmembrane ion transport in plants. Plant Physiol.

Chen, X., Lin, W.H., Wang, Y., Luan, S., Xue, H.W., 2008. An inositol polyphosphate 5-phosphatase functions in PHOTOTROPIN1 signaling in *Arabidopis* by altering cytosolic Ca^{2+}. Plant Cell 20, 353–366.

Edel, K.H., Marchadier, E., Brownlee, C., Kudla, J., Hetherington, A.M., 2017. The evolution of calcium-based signalling in plants. Curr. Biol. 27, R667–R679.

Freed, C., Adepoju, O., Gillaspy, G., 2020. Can inositol pyrophosphates inform strategies for developing low phytate crops? Plants 9, 115.

Gilroy, S., Read, N.D., Trewavas, A.J., 1990. Elevation of cytoplasmic calcium by caged calcium or caged inositol trisphosphate initiates stomatal closure. Nature 346, 769–771.

Hedrich, R., Kreuzer, I., 2023. Demystifying the Venus flytrap action potential. New Phytol.

Kisnierienė, V., Ditchenko, T.I., Kudryashov, A.P., Sakalauskas, V., Yurin, V.M., Rukšėnas, O., 2012. The effect of acetylcholine on Characeae K^+ channels at rest and during action potential generation. Cent. Eur. J. Biol. 7, 1066–1075.

Kisnieriene, V., Lapeikaite, I., Pupkis, V., Beilby, M.J., 2019. Modeling the action potential in Characeae *Nitellopsis obtusa*: effect of saline stress. Front. Plant Sci. 10, 82.

Koselski, M., Hoernstein, S.N.W., Wasko, P., Reski, R., Trebacz, K., 2023. Long-distance electrical and calcium signals evoked by hydrogen peroxide in *Physcomitrella*. Plant Cell Physiol. 64, 880–892.

Koselski, M., Pupkis, V., Hashimoto, K., Lapeikaitė, I., Hanaka, A., Wasko, P., Plukaitė, E., Kuchitsu, K., Kisnieriene, V., Trębacz, K., 2021. Impact of mammalian two-pore channel inhibitors on long-distance electrical signals in the Characean macroalga *Nitellopsis obtusa* and the early terrestrial liverwort *Marchantia polymorpha*. Plants 10, 647.

Koselski, M., Wasko, P., Derylo, K., Tchorzewski, M., Trebacz, K., 2020. Glutamate-induced electrical and calcium signals in the moss *Physcomitrella patens*. Plant Cell Physiol. 61, 1807–1817.

Krinke, O., Novotná, Z., Valentová, O., Martinec, J., 2007. Inositol trisphosphate receptor in higher plants: is it real? J. Exp. Bot. 58, 361–376.

Krol, E., Dziubinska, H., Stolarz, M., Trebacz, K., 2006. Effects of ion channel inhibitors on cold-and electrically-induced action potentials in Dionaea muscipula. Biol. Plant. 50, 411–416.

Król, E., Dziubińska, H., Trębacz, K., 2010. What do plants need action potentials for? In: DuBois, M.L. (Ed.), Action Potential. Nova Science Publishers, Inc., pp. 1–26

Krol, E., Dziubinska, H., Trebacz, K., Koselski, M., Stolarz, M., 2007. The influence of glutamic and aminoacetic acids on the excitability of the liverwort Conocephalum conicum. ARTICLE IN PRESS J. Plant Physiol. 164, 773–784.

Lapeikaitė, I., Dragūnaitė, U., Pupkis, V., Rukšėnas, O., Kisnierienė, V., 2019. Asparagine alters action potential parameters in single plant cell. Protoplasma 256, 511–519.

Lapeikaitė, I., Pupkis, V., Neniškis, V., Rukšėnas, O., Kisnierienė, V., 2020. Glutamate and NMDA affect cell excitability and action potential dynamics of single cell of macrophyte *Nitellopsis obtusa*. Funct. Plant Biol. 47, 1032–1040.

Larkin, D.J., Monfils, A.K., Boissezon, A., Sleith, R.S., Skawinski, P.M., Welling, C.H., Cahill, B.C., Karol, K.G., 2018. Biology, ecology, and management of starry stonewort (*Nitellopsis obtusa*; Characeae): a Red-listed Eurasian green alga invasive in North America. Aquat. Bot.

Lemtiri-Chlieh, F., MacRobbie, E.A.C., Brearley, C.A., 2000. Inositol hexakisphosphate is a physiological signal regulating the K^+-inward rectifying conductance in guard cells. Proc. Natl. Acad. Sci. 97, 8687–8692.

Lemtiri-Chlieh, F., Macrobbie, E.A.C., Webb, A.A.R., Manison, N.F., Brownlee, C., Skepper, J.N., Chen, J., Prestwich, G.D., Brearley, C.A., 2003. Inositol hexakisphosphate mobilizes an endomembrane store of calcium in guard cells. Proc. Natl. Acad. Sci. 100, 17–21.

Levchenko, V., Konrad, K.R., Dietrich, P., Roelfsema, M.R.G., Hedrich, R., 2005. Cytosolic abscisic acid activates guard cell anion channels without preceding Ca^{2+} signals. Proc. Natl. Acad. Sci. USA 102, 4203–4208.

Lunevsky, V.Z., Zherelova, O.M., Vostrikov, I.Y., Berestovsky, G.N., 1983. Excitation of Characeae cell membranes as a result of activation of calcium and chloride channels. J. Membr. Biol. 72, 43–58.

Meimoun, P., Vidal, G., Bohrer, A.S., Lehner, A., Tran, D., Briand, J., Bouteau, F., Rona, J. P., 2009. Intracellular Ca^{2+} stores could participate to abscisic acid-induced depolarization and stomatal closure in *Arabidopsis thaliana*. Plant Signal. Behav. 4, 830–835.

Mousavi, S.A.R., Chauvin, A., Pascaud, F., Kellenberger, S., Farmer, E.E., 2013. GLUTAMATE RECEPTOR-LIKE genes mediate leaf-to-leaf wound signalling. Nature 500, 422–426.

Munnik, T., Testerink, C., 2009. Plant phospholipid signaling: "in a nutshell". J. Lipid Res. 50, S260–S265.

Munnik, T., Vermeer, J.E.M., 2010. Osmotic stress-induced phosphoinositide and inositol phosphate signalling in plants. Plant Cell Environ. 33, 655–669.

Navickaite, A., Pupkis, V., Kalnaityte-Vengeliene, A., Lapeikaite, I., Kisnieriene, V., Bagdonas, S., 2024. Combining *Nitellopsis obtusa* autofluorescence intensity and F680/F750 ratio to discriminate responses to environmental stressors. Methods Appl. Fluoresc. 12, 045003.

Nishiyama, T., Sakayama, H., de Vries, J., Buschmann, H., Saint-Marcoux, D., Ullrich, K. K., Haas, F.B., Vanderstraeten, L., Becker, D., Lang, D., Vosolsobě, S., Rombauts, S., Wilhelmsson, P.K.I., Janitza, P., Kern, R., Heyl, A., Rümpler, F., Villalobos, L.I.A.C., Clay, J.M., Skokan, R., Toyoda, A., Suzuki, Y., Kagoshima, H., Schijlen, E., Tajeshwar, N., Catarino, B., Hetherington, A.J., Saltykova, A., Bonnot, C., Breuninger, H., Symeonidi, A., Radhakrishnan, G.V., Van Nieuwerburgh, F., Deforce, D., Chang, C., Karol, K.G., Hedrich, R., Ulvskov, P., Glöckner, G., Delwiche, C.F., Petrášek, J., Van de Peer, Y., Friml, J., Beilby, M., Dolan, L., Kohara, Y., Sugano, S., Fujiyama, A., Delaux, P.M., Quint, M., Theißen, G., Hagemann, M., Harholt, J., Dunand, C., Zachgo, S., Langdale, J., Maumus, F., Van Der Straeten, D., Gould, S.B., Rensing, S.A., 2018. The *Chara* genome: secondary complexity and implications for plant terrestrialization. Cell 174, 448–464.e24.

Novikova, E.M., Vodeneev, V.A., Sukhov, V.S., 2017. Mathematical model of action potential in higher plants with account for the involvement of vacuole in the electrical signal generation. Biochem. (Mosc.) Suppl. Ser. A Membr. Cell Biol. 11, 151–167.

Othmer, H.G., 1997. Signal transduction and second messenger systems. In: Othmer, H. G., Adler, F.R., Lewis, M.A., Dallon, J. (Eds.), Case Studies in Mathematical Modeling–Ecology, Physiology and Cell Biology. Prentice Hall, Englewood Cliffs, NJ, pp. 101–128.

Perera, I.Y., Hung, C.Y., Brady, S., Muday, G.K., Boss, W.F., 2006. A universal role for inositol 1,4,5-trisphosphate-mediated signaling in plant gravitropism. Plant Physiol. 140, 746–760.

Pottosin, I., Dobrovinskaya, O., 2014. Non-selective cation channels in plasma and vacuolar membranes and their contribution to K^+ transport. J. Plant Physiol. 171, 732–742.

Pottosin, I., Wherrett, T., Shabala, S., Schroeder, J., 2009. SV channels dominate the vacuolar Ca2+ release during intracellular signaling.

Pupkis, V., Buisas, R., Lapeikaite, I., Kisnieriene, V., 2021. Using plant cells of *Nitellopsis obtusa* for biophysical education. Biophysicist 2, 18–29.

Pupkis, V., Lapeikaite, I., Kavaliauskas, J., Trębacz, K., Kisnieriene, V., 2022. Certain calcium channel inhibitors exhibit a number of secondary effects on the physiological properties in *Nitellopsis obtusa*: a voltage clamp approach. Funct. Plant Biol.

Raboy, V., 2003. myo-Inositol-1,2,3,4,5,6-hexakisphosphate. Phytochemistry 64, 1033–1043.

Scherzer, S., Böhm, J., Huang, S., Iosip, A.L., Kreuzer, I., Becker, D., Heckmann, M., Al-Rasheid, K.A.S., Dreyer, I., Hedrich, R., 2022a. A unique inventory of ion transporters poises the Venus flytrap to fast-propagating action potentials and calcium waves. Curr. Biol. 32, 4255–4263 e5.

Scherzer, S., Huang, S., Iosip, A., Kreuzer, I., Yokawa, K., AL-Rasheid, K.A.S., Heckmann, M., Hedrich, R., 2022b. Ether anesthetics prevents touch-induced trigger hair calcium-electrical signals excite the Venus flytrap. Sci. Rep. 12, 2851.

Shiina, T., Tazawa, M., 1987. Ca^{2+}-activated Cl^- channel in plasmalemma of *Nitellopsis obtusa*. J. Membr. Biol. 99, 137–146.

Shimmen, T., 2007. The sliding theory of cytoplasmic streaming: fifty years of progress. J. Plant Res. 120, 31–43.

Sukhov, V., Sukhova, E., Vodeneev, V., 2019. Long-distance electrical signals as a link between the local action of stressors and the systemic physiological responses in higher plants. Prog. Biophys. Mol. Biol. 146, 63–84.

Tan, X., Calderon-Villalobos, L.I.A., Sharon, M., Zheng, C., Robinson, C.V., Estelle, M., Zheng, N., 2007. Mechanism of auxin perception by the TIR1 ubiquitin ligase. Nature 446, 640–645.

Tazawa, M., Kikuyama, M., 2003. Is Ca^{2+} release from internal stores involved in membrane excitation in Characean cells? Plant Cell Physiol. 44, 518–526.
Tsutsui, I., Ohkawa, T., Nagai, R., Kishimoto, U., 1987a. Role of calcium ion in the excitability and electrogenic pump activity of the *Chara corallina* membrane: II. effects of La^{3+}, EGTA, and calmodulin antagonists on the current-voltage relation. J. Membr. Biol. 96, 75–84.
Tsutsui, I., Ohkawa, T., Nagai, R., Kishimoto, U., 1987b. Role of calcium ion in the excitability and electrogenic pump activity of the *Chara corallina* membrane: I. Effects of La^{3+}, verapamil, EGTA, W-7, and TFP on the action potential. J. Membr. Biol. 96, 65–73.
Vodeneev, V., Katicheva, L.A., Sukhov, V.S., 2016. Electrical signals in higher plants: mechanisms of generation and propagation. Biophysics 61, 505–512 (Russian Federation).
Wacke, M., Thiel, G., 2001. Electrically triggered all-or-none Ca^{2+}-liberation during action potential in the giant alga *Chara*. J. Gen. Physiol. 118, 11–22.
Wacke, M., Thiel, G., Hütt, M.T., 2003. Ca^{2+} dynamics during membrane excitation of green alga *Chara*: model simulations and experimental data. J. Membr. Biol. 191, 179–192.
Williamson, R., Ashley, C.C., 1982. Free Ca^{2+} and cytoplasmic streaming in the alga *Chara*. Nature 296, 647–651.
Xiong, L., Lee, B.H., Ishitani, M., Lee, H., Zhang, C., Zhu, J.K., 2001. FIERY1 encoding an inositol polyphosphate 1-phosphatase is negative regulator of abscisic acid and stress signaling in Arabidopsis. Genes Dev. 15, 1971–1984.
Zhang, J., Vanneste, S., Brewer, P.B., Michniewicz, M., Grones, P., Kleine-Vehn, J., Löfke, C., Teichmann, T., Bielach, A., Cannoot, B., Hoyerová, K., Chen, X., Xue, H.W., Benková, E., Zažímalová, E., Friml, J., 2011. Inositol trisphosphate-induced Ca^{2+} signaling modulates auxin transport and pin polarity. Dev. Cell 20, 855–866.
Zherelova, O.M., 1989. Activation of chloride channels in the plasmalemma of *Nitella syncarpa* by inositol 1,4,5-trisphosphate. FEBS Lett. 249, 105–107.
Zherelova, O.M., Kataev, A.A., Grishchenko, V.M., Knyazeva, E.L., Permyakov, S.E., Permyakov, E.A., 2009. Interaction of antitumor α-lactalbumin-oleic acid complexes with artificial and natural membranes. J. Bioenerg. Biomembr. 41, 229–237.